Solid State Science and Technology, Vol. 21, No 1 & 2 (2013) 1-9
ISSN 0128-7389

EXPERIMENTAL STUDY TOWARDS FABRICATION OF SPRAY-DRIED PHOTOCATALYTIC TITANIUM DIOXIDE FILMS FOR WATER TREATMENT

Ahmad Zaki Shaari*, Mat Tamizi Zainuddin, Shamsul Azrolsani Abdul Aziz Nazri, Shahrul Nizam Md. Salleh and Mohamad Zahid Abdul Malek

Advanced Materials Research Centre (AMREC), SIRIM Berhad
Lot 34, Jalan Hi-Tech 2/3, Kulim Hi- Tech Park, 09000 Kulim, Kedah, Malaysia

**Corresponding author: zaki@sirim.my*

ABSTRACT

Doped TiO_2 were milled and then processed into powder using a spray dryer. The powder was dried overnight and then heat treated (calcined) at different temperatures for 4 hours. Characterization of doped TiO_2 was done using Field Emission Scanning Electron Microscope for size and morphology determination; X-Ray Diffractometer for crystallinity analysis; and FT Raman Spectrometer for Raman spectroscopic analysis. As calcination temperature went up, rutile phase increased with increased crystallite size in commercial (Degussa P25) TiO_2 but it was not observed in the doped sample. The crystallite size and diffraction peak intensity of the doped (anatese) TiO_2 increased as calcination temperature went up. Diffraction peaks for talc disappeared after milling (i.e grinding process). Two new RAMAN bands started to emerge at 1926 and 1498 cm^{-1} starting at temperature 750°C and showed significant peaks at 950°C due to presence of talc or its constituents in the doped sample. This requires further study and investigation.

Keywords: Water Treatment; Photo Catalys; Titanium Dioxide; Spray Drying; Grinding Process;

INTRODUCTION

Photocatalytic titanium dioxide or titania or titanium (IV) oxide (TiO_2) is used to decontaminate water supply from bacteria, viruses and organic compounds [1]. TiO_2 is also utilized in application such as photocatalytic degradation of various contaminants in waste air or wastewater treatment [2, 3]

Two crystalline forms of TiO_2 have photocatalytic activity; anatese and rutile. Both have a band gap of 3.2 eV and 3.0 eV respectively. Even though anatese has been found to be the most active form, it had shown a sharp decrease in activity above 385 nm wavelength of light. In addition to the phase composition, parameters such as surface area, crystallite size and pore size are important factors influencing the photocatalytic performance of TiO_2 [4, 5, 6].

TiO_2 photo catalyst can also be immobilized onto a fixed solid support in order to avoid separation process but there is inherently a decrease in the surface area available for reaction. The reaction occurs at the liquid-solid interface and the overall rate may be limited to mass transport of the pollutant to the catalyst surface and thus the overall removal efficiency also decreases. Gel-derived TiO_2–SiO_2 mixed oxide-based photocatalysts was used to reduce CO_2 with H_2O to fuels under natural sunlight by using a solar concentrator [7].

The performance of any removal systems may be improved through supporting the TiO_2 nanoparticles in matrices that increase the effective dwelling time of pollutants in the proximity of the photocatalyst. A porous material, where the compound can penetrate a porous structure, ensures that the pollutants reside there long enough for the catalyst to work. This knowledge prompted us to examine further clay materials. Clays often present a large surface area for adsorption of organic pollutants, and can also interact directly with pollutants through redox and acid-base interactions [8].

MATERIALS AND METHODS

Powdered samples were prepared by mixing Titanium (IV) Oxide (Sigma-Aldrich) and a small quantity of talc. The mixed sample was then poured inside a bottle containing distilled water. Alumina ball was added to assist grinding and mixing process. The bottle was then rotated at low speed for 24 hours using Ball Mill machine.

The sample was recovered by centrifugation (spray dryer LABPlant SD-05), and dried at 70°C for 8 hours. The TiO_2 particles were calcined at 750, 850 and 950°C with a heat rate of 3°C min−1 and a keeping time of 4 hours.

Characterization of samples was done using Field Emission Scanning Electron Microscope (FESEM, LEO 1525, 30kV) for size and morphology determination; X-Ray Diffractometer (XRD, Bruker, D8) for crystallinity analysis; and FT Raman Spectrometer (Renishaw, RE04) for Raman spectroscopic analysis.

X-ray diffraction patterns were recorded using CuKα radiation in the step-scan mode with a 2θ range of 20° to 90°. The scanning was performed in steps of 0.040° 2θ with an interval of 1 sec. The crystallite size and the relative amounts of the anatase and rutile phase were calculated from the (101) reflection of anatase and the (110) reflection of rutile. The crystallite size of anatase and rutile phase was calculated using the Scherrer's equation [5]:

$$t = \frac{k\lambda}{s\cos\theta} \quad (1)$$

where t is the crystallite size, λ is the wavelength of the X-ray radiation (CuKα = 0.15406 nm, 40 kV, 40mV), k is a constant that was set to 0.94, θ is the diffraction angle, and s is the line width at half maximum height.

The mass fractions of anatase present in TiO_2 were calculated using the equation given below [9]:

$$Anatese(\%) = 100\left[\frac{0.79I_A}{I_R + 0.79I_A}\right] \quad (2)$$

Where I_A and I_R is the diffraction peak intensity of the anatase (101) phase and rutile (110) phase respectively

RESULTS

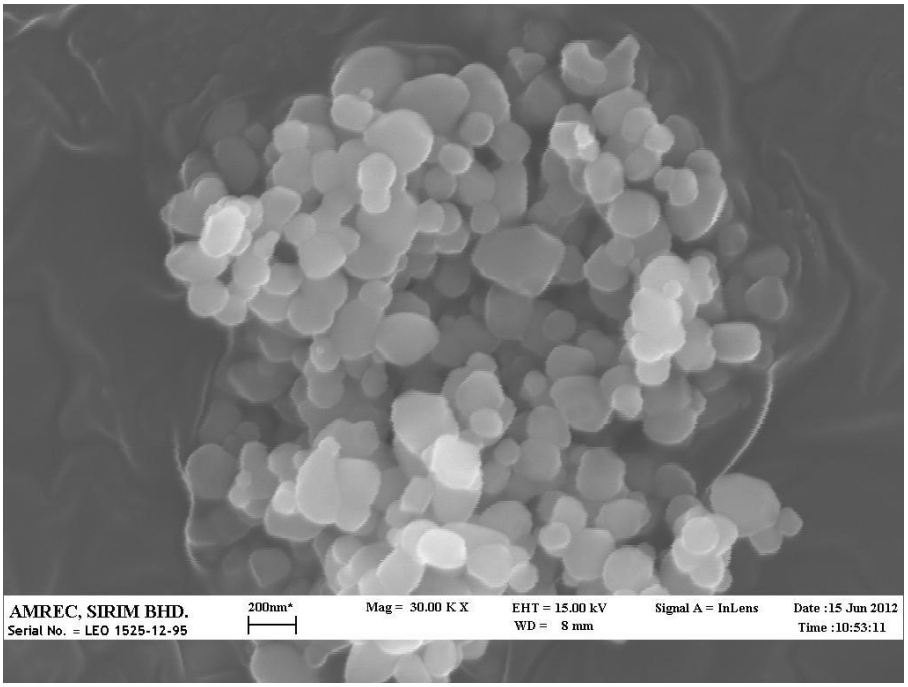

(a)

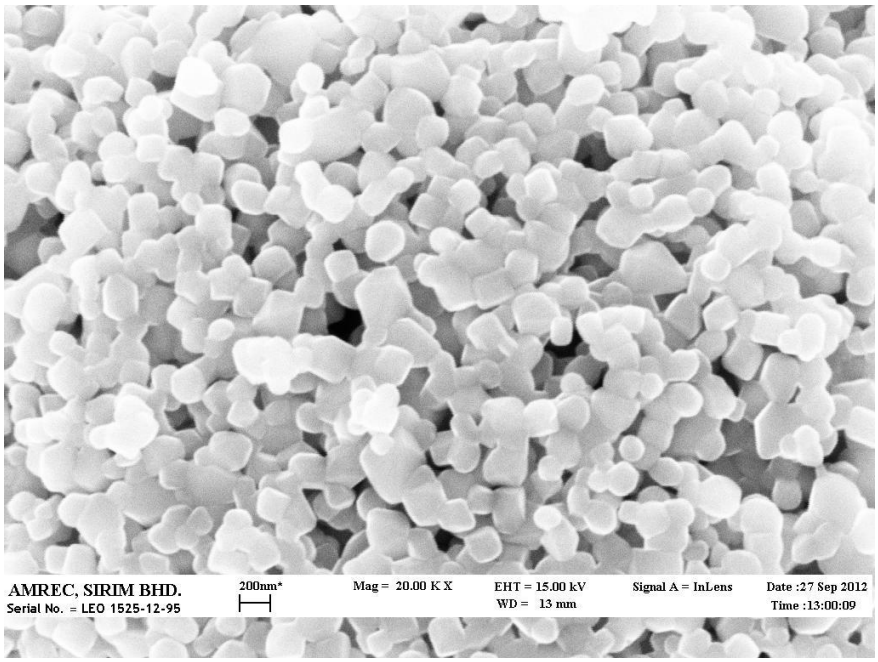

(b)

Figure 1: FESEM images of of the doped sample (anatese Titania Titanium (IV) Oxide, CAS-Nr: 13463-67-7 and talc) calcined at temperatures (a) 750°C; (b) 850°C

Figure 1 show FESEM images of the (TiO_2 + Talc) sample calcined at 750°C and 950°C.

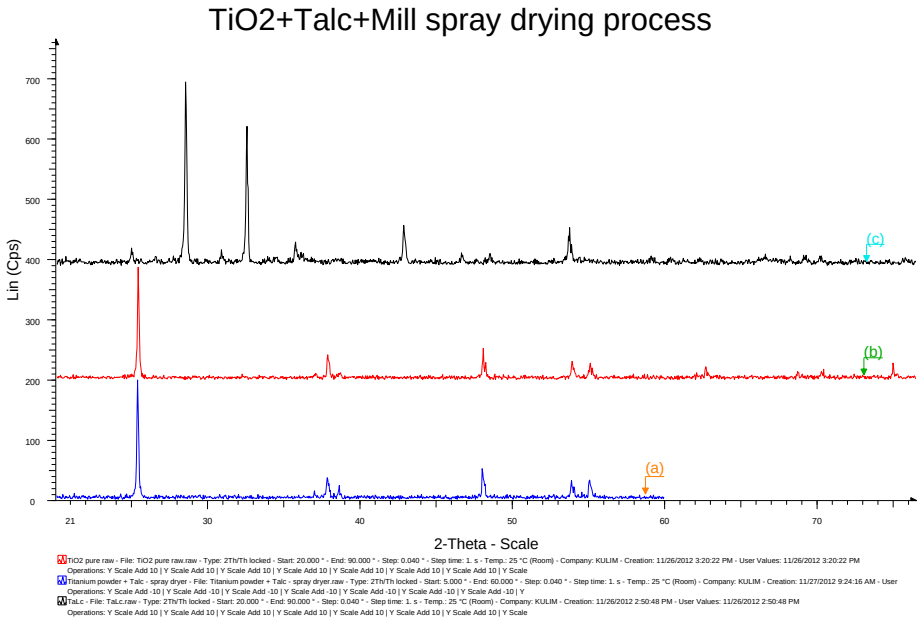

Figure 2: XRD patterns of the samples [(a) doped or (TiO_2 + talc) after grinding process, (b) raw anatese (undoped) TiO_2 and (c) raw Talc]

The XRD peak at 2θ = 25.40° (Figure 2(a) and 2(b)) is known to be the characteristic peaks of anatase (101) crystal phases of TiO_2 [4, 10]. The XRD peaks at 2θ = 28.52° (Figure 2(c)) is known to be the characteristic peaks of anatase (006) crystal phases of Talc [11]. However, the anatese peak of talc is not observed in the (TiO_2 + talc) sample (a) after milling (i.e grinding) process. The XRD peaks at 2θ = 25.16° and 2θ =27.50°

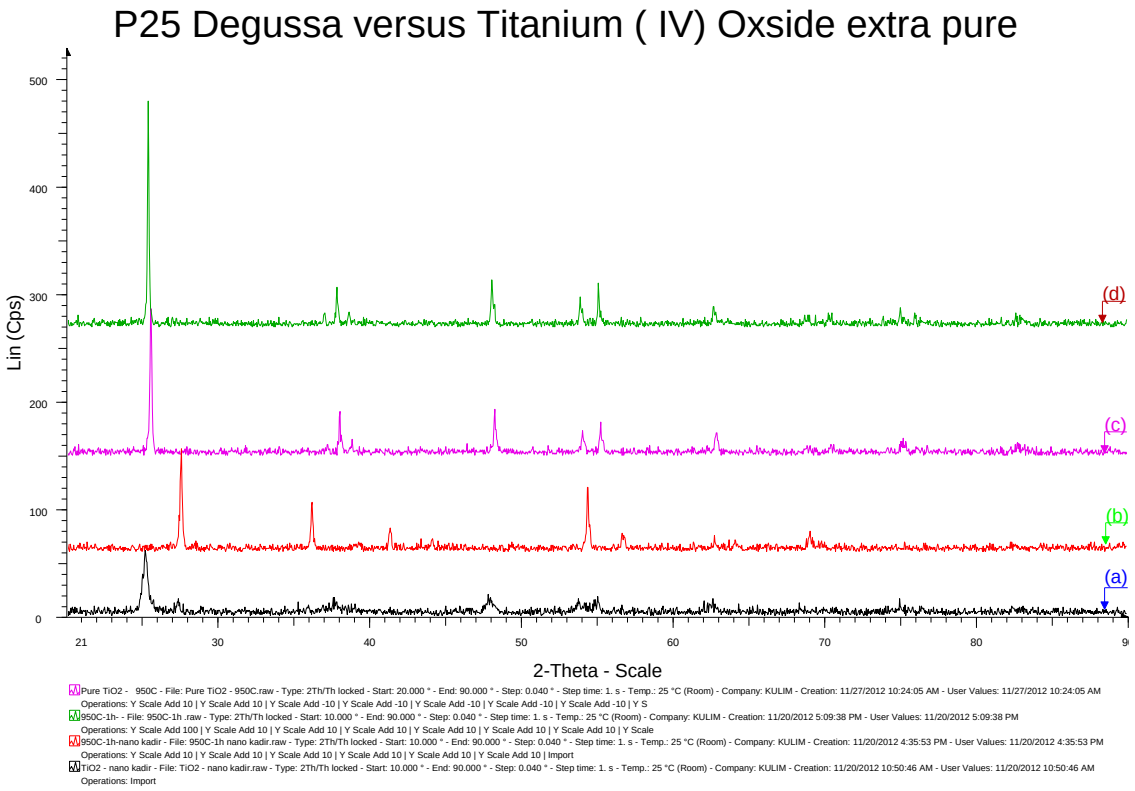

Figure 3: XRD patterns of the samples; (a) raw (anatese 75%, rutile 25%) Degussa P25; (b) Degussa P25 after calcining at 950 °C, and turns to rutile completely; (c) (anatese TiO_2) undoped sample after calcining at 950°C; and (d) (TiO_2 + talc) doped sample after 950°C shows increasing anatese intensity

(Figure 3(a) and 3(b) respectively) are known to be the characteristic peaks of anatase (101) and rutile (110) crystal phases, respectively of Degussa P25 [4]. The (TiO_2 + talc) sample after heat treated at 950°C (Figure 3(d)) shows increasing anatese intensity peak (101) as compared peak for pure TiO_2 (Figure 3 (c)). There is not much difference in term of phase changes in both samples.

Table 1: Different samples show difference crystallite sizes

Sample	Anatese Peak	Max Intensities (Cps)	Crystallite Size (nm)
Degussa P25 (75% Anatese, 25% Rutile)	25.16	59	21
Undoped TiO_2 (100% Anatese)	25.40	187	72
Undoped TiO_2 (750°C)	25.33	118	41
Undoped TiO_2 (950°C)	25.50	140	58
TiO_2 + Talc (750°C)	25.35	222	60
TiO_2 + Talc (850°C)	25.22	204	71
TiO_2 + Talc (950°C)	25.33	212	75

The crystallite size for the (TiO_2 + talc) sample was consistently measured to be in between 60 – 75 nm (Table 1). Crystallite size increased with increasing calcination temperature, showing substantial increase at the temperature range between 500°C and 1,000°C [4,5,10].

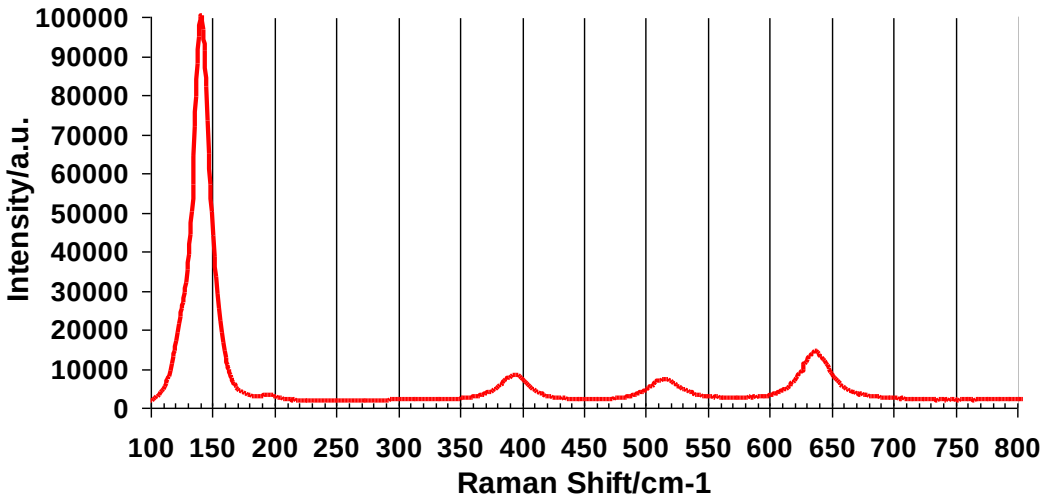

Figure 4: Raman spectra of pure titania

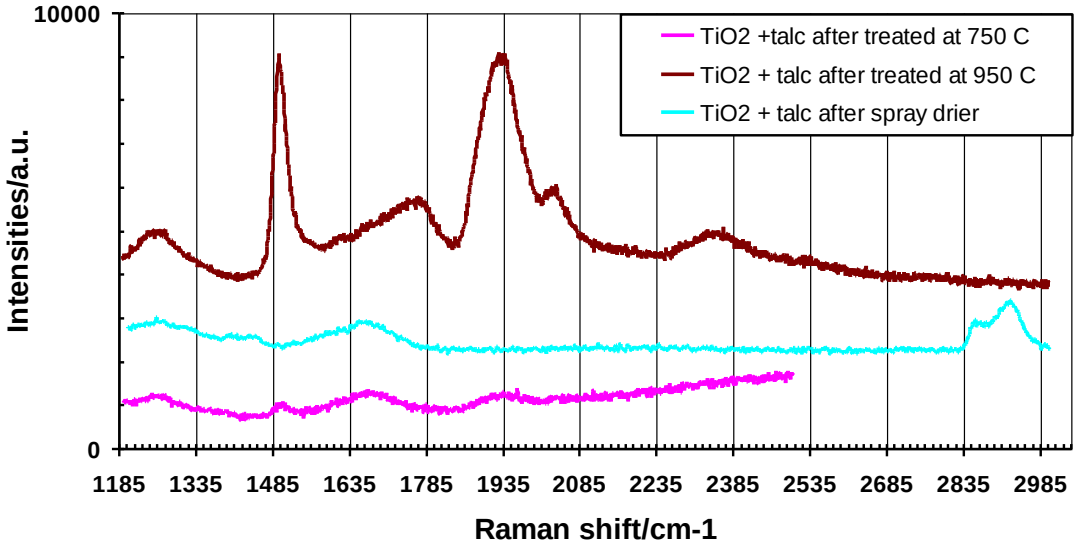

Figure 5: Raman shift of the (TiO_2+ talc) doped sample before and after calcination

The anatase and rutile phases of TiO_2 can be sensitively identified by Raman spectroscopy based on their Raman spectra. The anatese phase (Figure 4) of TiO_2 shows similar Raman bands at 142, 195, 394, 515 and 638 cm^{-1} [12,13]. Figure [2(a) and 3(d)] and Figure 5 shows XRD patterns and RAMAN sprectra respectively, of a similar sample (TiO_2 + talc mixture) before and after calcination process. Raman bands at 2858 and 2926 cm^{-1} are shown in Figure 5 for (TiO_2 + talc) sample before heating while the bands disappeared completely after calcination temperature 950°C. Two new RAMAN bands start to emerge at 1926 and 1498 cm^{-1} starting at 750°C and show significant peaks at 950°C.

DISCUSSION

The phase transformation from anatase to rutile progressively proceeds at the elevated temperatures [4,10,13]. The diffraction peaks of anatese phase of Degussa P25 disappeared at 950°C, which indicated phase transformation in which the anatase phase completely changed into the rutile phase. However, this was not observed in the (anatese TiO_2 + talc) doped samples at similar temperature. Anatase peaks were simply not affected (in term of changing to rutile phase as its peak (anatese) intensity increased (Figure 3(d) and Table 1). However, the peak (anatese) intensity of undoped samples decreased (Table 1) even though its rutile peak was not yet observed at 950°C. The crystallite size increased with increasing calcination temperature, as similarly found in other literatures stated above.

These findings show that if the direct contact between anatase particles is prevented, the phase transformation could be retarded or prohibited because of the rutile phase could not nucleate at the interfaces of the defect sites on the surface of the anatase particles.

These particles are assumed to play an important role in the phase transformation of TiO_2 [13]. When the defect sites of the anatase particle react with a neighboring anatase particle, the rutile phase formation may start at these sites.

Talc or its constituents can easily react with the defect sites of the anatase particles, and it can occupy or deactivate all the defect sites of the anatase particles. Two Raman bands at 2858 and 2926 cm^{-1} show the presence of hydroxyl group due to magnesium-silicate layer was disrupted during milling/grinding process. When the edge surfaces are exposed to atmosphere, brucite (Mg(OH)2) or even silica may absorbed water molecules and become covered with amphoteric surface hydroxyls, mainly in the form of silanol (-Si-OH), aluminol (-Al-OH) or magnesol (-Mg-OH) [14]. Pure talc is thermally stable up to 930°C, and loses its crystalline bound water (4.8%) between 930 and 970°C [15]. When the doped samples were heated up, two new RAMAN bands started to emerge at 1926 and 1498 cm^{-1} starting at temperature 750°C and showed significant peaks at 950°C due to presence of talc in the doped sample. This requires further study and investigation

Therefore, while the (TiO_2 + talc) doped samples could retain its anatase phase even when the calcination temperature was up to 950°C, it requires further investigations in terms of confirming what actually happens in RAMAN spectra in between 1100 and 3000 cm^{-1}.

CONCLUSION

We report a technique using a spray dryer to produce doped (talc) titanium dioxide powder after milling process. Two samples (doped TiO_2 and Degussa P25) were calcined at temperature 750, 850 and 950°C for 4 hours. Degussa P25 mixed phases (75% anatese + 25% rutile) showed complete phase transition to rutile at 950°C while doped (100% anatese) TiO_2 did not show any phase transition to rutile. Instead, diffraction peak (anatese) intensity and crystallite size increased as calcination temperature went up. Diffraction peaks for talc in the doped sample disappeared completely after milling (i.e grinding process). Two new RAMAN bands started to emerge at 1926 and 1498 cm^{-1} starting at temperature 750°C and showed significant peaks at 950°C due to presence of talc or its constituents in the doped sample. This requires further study and investigation.

Acknowledgement

REFERENCES

[1]. Fujishima A., Hashimoto K., Watanabe T. *Fundamentals and Applications Tokyo,* (1999) 14

[2]. Chong M.N., Jin B., Chow C.W.K, Saint C. *Water Research* **44** (2010) 2997-3027

[3]. Thiruvenkatachari R., Vigneswaran S., Moon S. I. *Korean J. Chem. Eng.*, **25** (1)

(2008) 64-72
[4]. Antony Raj K. J., Viswanathan V. *Indian Journal of Chemistry*, 28(A) (2009) 1378-1382
[5]. Kim D. S., Han S. J., Kwak S.Y. *Journal of Colloid and Interface Science*, **316** (1) (2007) 85 – 91
[6]. Zhang Q., Gao L., Guo *J. Applied Catalysis B, Env.* **26** (2000) 207–215
[7]. Nguyen TV., Jeffrey Wu C.S. *Solar Energy Materials & Solar Cells*, **92** (2008) 864–872
[8]. Nagendrappa G. *Resonance* (2002) 64-77
[9]. Thompson T. L. and Yates J. T. *Chemical Review* **106** (2006) 4428
[10]. Han Y., Kim H. S., Kim H. *Journal of Nanomaterials* (2012) 1-10
[11]. Yang H., Du C. F. *Applied Clay Science* **31** (2006) 290-297
[12]. Tsai, S.J.; Cheng S. *Cataysis Today* **33** (1997) 227-237
[13]. Zhang J., Li M., Feng Z., Chen J., Li C. *The Journal of Physical Chemistry B,* **110** (2) (2006) 927–935
[14]. Yariv S. *Modern Approches in Wettability,* (1992) 279-326
[15]. Wesolowski M.; *Thermochimica Acta,* (1984) 395-421